Electronic structure, phase stability, and chemical ordering of the ω phase in a Ti_3Al_2X (X=Nb,V) alloy

M. Sanati,[1,2,*] D. West,[1] and R. C. Albers[2]
[1]*Physics Department, Texas Tech University, Lubbock, Texas 79409-1051, USA*
[2]*Theoretical Division, Los Alamos National Laboratory, Los Alamos, New Mexico 89404, USA*
(Received 12 July 2007; published 2 November 2007)

The phase stability of $B2$ Ti_3Al_2X (X=Nb or V) and slightly rearranged atomic structures is examined by first-principles calculations. The ground-state energy calculations show instability in some of the Ti_3Al_2X configurations against the ω structure type of atomic displacement. We use electronic density of states and Mulliken population analysis to understand the hybridization between the atoms and the electronic origin of the stability or instability of each system. In order to estimate the strength of each bond, the heats of formation for several compounds are calculated. We find that the strength of the transition metal–Al bond increases from V to Nb to Ti, with Ti-V and Ti-Nb being weakly unstable. By examining several atomic configurations, it is shown that the stability of each structure is directly related to the number of Ti-Al bonds in each configuration. It is confirmed that the formation of the ω phase in Ti_3Al_2X is a combined displacive-replacive transformation. The crystal structure parameters, such as lattice constants and bulk modulus, are calculated and compared with available experimental data.

DOI: 10.1103/PhysRevB.76.174101 PACS number(s): 64.70.Kb, 61.50.Ks

I. INTRODUCTION

In the area of materials physics, the mechanisms for diffusionless (or continuous) phase transitions into metastable-like states are of considerable interest. Such systems are a simpler paradigm for complexity in materials. In this paper, we focus on the stability of the underlying bcc phase of Ti_3Al_2Nb and Ti_3Al_2V alloys and the importance of the chemical ordering in promoting the ω-phase stability or instability in these systems. Our emphasis will be on the zero-temperature electronic structure, hybridization, and bonding in these systems to provide a detailed account of the instability. Understanding these basics is a first step before attempting a more complex description (including entropy) of the nonequilibrium nature of the phase transformations in these types of systems.

Over the past two decades, considerable effort has been expended in producing alloys based on titanium aluminides because of their low density and good high-temperature properties. They also show improved oxidation resistance over the conventional Ti alloys. The most important limitation of these alloys lies in their low-temperature brittleness. The addition of a third element[1] not only affects their properties but also how they can be processed. An increasing amount of data is now available concerning the phase transformations in the Ti-Al-Nb (Refs. 2–8) and Ti-Al-V (Refs. 9–13) systems. For these systems, various phase transitions have been observed. However, among the different observed phases particular attention must to be paid to the ω-type phase, since this type of phase is often detrimental to ductility. Studying the occurrence and stability of the ω phase may ultimately be used to prevent its presence in microstructure thereby preserving the mechanical properties. On the other hand, the high-strength characteristics of the ω phase may be useful in applications which require a high-temperature structural material.

The mechanism generally assumed for the bcc $\rightarrow \omega$ transformation is the collapse of the $\{111\}_\beta$ plane due to a $(2/3)\times\langle 111\rangle_\beta$ longitudinal displacement wave.[14] Thus, when the ω phase is created, two neighboring (111) plane move toward each other by a displacement in the [111] direction, while each third plane remains unmoved. This type of transformation is called displacive because it involves cooperative movement over small distances which are fractions of lattice translation vectors. In contrast, a diffusion-controlled nucleation and growth transformation occurs via atomic diffusion.

The formation of the trigonal (incomplete) ω phase (ω'') in Ti-Al-Nb (Refs. 2–5) and Ti-Al-V (Refs. 11–13) alloys have been reported by several experiments. Bendersky *et al.*[2] reported a sequence of phase transitions: chemically disordered bcc $(A2)\rightarrow$ ordered $B2\rightarrow\omega''\rightarrow B8_2$, for the $Ti_3Al_{2.25}Nb_{0.75}$ alloy. Evidently because ω'' is metastable, the equilibrium transformation $B2$ $(Pm\bar{3}m)\rightarrow B8_2$ $(P6_3/mmc)$ is strongly first order due to symmetry, since $P6_3/mmc$ is not a subgroup of $Pm\bar{3}m$. The observed path, $B2\rightarrow\omega''\rightarrow B8_2$, traverses a state of minimum symmetry $(\omega'', P\bar{3}m1)$ that is a subgroup of both $Pm\bar{3}m$ and $P6_3/mmc$. This space group of minimum symmetry is the intersection of the parent and product space groups. The formation of ω'' as an intermediate metastable phase provides a continuous structural path for the alloy to accomplish the $B2$ to $B8_2$ transition. In the alloy with chemical composition around the $Ti_3Al_{2.1}V_{0.9}$ similar transformations have been observed.[10,12,13] However, the ordered ω phase is trigonal with a space group $P\bar{3}m1$ and transformation to the $B8_2$ phase has not been seen.[13]

In the Ti-Al-Nb system, the $B2$ occupancy reported by Banerjee *et al.*[15] showed that Ti tends to occupy one site while Al and Nb tend to occupy the other site. The measured site occupancies of the ω'' phase indicate that the first change in chemical order is the transfer of Nb atoms out of the collapsing planes (Fig. 1) into stationary ones.[2] It is suggested that the absence of the Nb atoms from the collapsing planes is because of the strong interaction between Ti and Al atoms (due to the considerably large negative heat of mixing

 ©2007 The American Physical Society

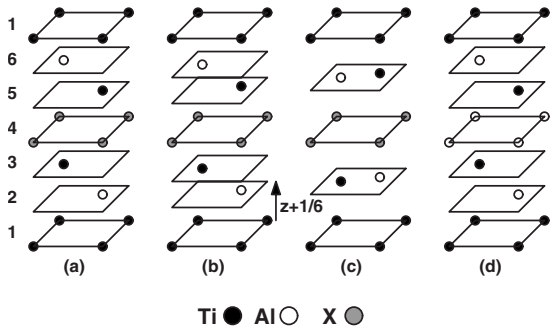

FIG. 1. (a) Stacking of the (111) planes of the bcc Ti_3Al_2X structure (BOT), (b) ω'' structure (partial collapse of the planes), (c) ω structure (full collapse of two of the planes), and (d) $B2$ TiAl structure. The parameter z is a measure of the movement of the second plane. When all planes are equidistant, $z=0$, and the first plane is at a distance $1/6$ of c/a above the lowest plane. As the ω shuffle progresses to completion, this plane moves up by $1/12$ of c/a (the plane above it simultaneously moves down by $1/12$ of c/a).

between them).[2,11,13] Therefore, transition metal (TM)–Al interactions are the origin of both the $A2 \rightarrow B2$ ordering and the ω-phase formation in the $B2$ phase of TiAl-X (X =Nb, V) system.

So far there is no theoretical study on Ti-Al-X (around the mentioned compositions) in the $B2$ and ω phases and the number of experimental studies are also limited. Reliable information, such as crystal lattice parameters, bulk moduli, heats of formation, and electronic densities of states are also lacking. Furthermore, there is very little understanding of the stability of the underlying bcc structure against the ω-type distortions from the electronic perspective.

The present work is concerned with the electronic origin of the ω-phase formation in Ti_3Al_2X (X=Nb, V) system, both chemical (replacive) and displacive transitions and the strong coupling between the two. Two different first-principles methods are used for calculating crystal parameters, energetics of structures, charge densities, and Mulliken overlap population analysis (MOPA). This paper is organized as follows: Section II discusses the details of calculations. Section III contains the results for crystal parameters, MOPA, hybridization, heats of formation, and bond strengths of the different atomic pairs. Section IV deals with the stability of the underlying bcc and ω'' phases. The chemical ordering process in formation of the ω'' phase is discussed in Sec. V. A summary of our findings is presented in Sec. VI.

II. DETAILS OF CALCULATIONS

The present calculations have been carried out using two first-principles density-functional packages, VASP (Refs. 16–19) and SIESTA,[20,21] within the generalized gradient approximation to the exchange-correlation potential (Refs. 22 for VASP and 23 for SIESTA). We use SIESTA for the MOPA, while VASP is used for the rest of the calculations.

The VASP calculations use a plane-wave basis set and ultrasoft Vanderbilt-type pseudopotentials.[24] For transition metal pseudopotentials, the semicore p orbitals are included in valence. In the VASP approach, the solution of the generalized self-consistent Kohn-Sham equations is calculated using an efficient matrix-diagonalization routine based on a sequential band-by-band residual minimization method and Pulay-like charge density mixing.[25] We used a plane-wave basis cutoff at 304.7 eV for all structures. Electronic degrees of freedom were optimized with a conjugate gradient algorithm, and both cell constants and ionic positions are fully relaxed. The crystal is represented by a six-atom cell. A $7 \times 7 \times 5$ Monkhorst-Pack[26] mesh is used to sample the Brillouin zone.

The SIESTA calculations use norm-conserving pseudopotentials in the Troullier-Martins form[27] to remove the core regions from the calculations. The basis sets for the valence states are linear combinations of numerical atomic orbitals.[20,28,29] In the present calculations, we use double-ζ polarized basis sets (two sets of valence s and p's plus one set of d's). The charge density is projected on a real-space grid with an equivalent cutoff of 150 Ry to calculate the exchange-correlation and Hartree potentials.

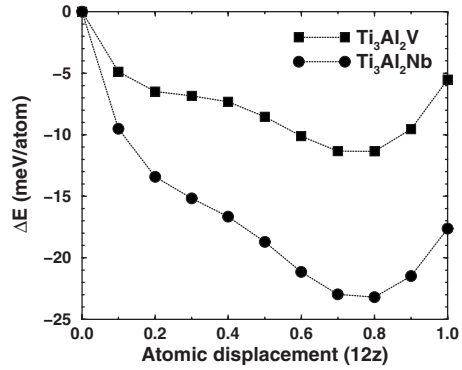

FIG. 2. Calculated total energy as a function of atomic displacement for Ti_3Al_2X system. Value of E_0 is equal to the energy of each BOT structure.

III. ELECTRONIC STRUCTURE, HYBRIDIZATION, AND BOND STRENGTH

To understand a crystal structure from first principles, it is first useful to determine the overall unit cell. The unit cell has six atoms for the Ti_3Al_2X system, as shown in Fig. 1. We constrained the c/a ratio to $\sqrt{6}/2$ (ideal value), and determined the lattice constant a. After studying all of the possible arrangements of the atoms in the six-atom unit cell within the bcc structure, we find that the atomic configuration in Fig. 1(a) has the lowest energy. [For convenience, from now on, the structure shown in Fig. 1(a) is referred to as the body center orthogonal ternary (BOT) structure.] Then, we varied the positions of the planes along $(111)_{bcc}$ and optimized the lattice parameters for each new configuration. Calculated total energy vs plane displacement z (where z is a dimensionless variable varying between 0 and $1/12$ in terms of the c/a unit) is shown in Fig. 2. The lattice with $z=0$ corresponds to a bcc structure. The complete ω phase is formed when $z=1/12$; for the other values of z, the structures are the "in-

TABLE I. Calculated values for atomic parameters of Ti_3Al_2X BOT and ω'' structures. The experimental parameters (given in parentheses) correspond to $Ti_3Al_{2.25}Nb_{0.75}$ (for BOT Ref. 3 and for ω'' Ref. 2) and $Ti_3Al_{2.1}V_{0.9}$ (Ref. 13) alloys.

	X			
	V BOT	Nb BOT	V ω''	Nb ω''
a (Å)	3.224 (3.179)	3.229 (3.247)	4.526	4.609 (4.555)
c (Å)			5.407	5.479 (5.542)
$z+1/6$			0.2306	0.2335 (0.2245)
B (GPa)	121.5	119.4	117.5	121.4
N_{E_f} (states/eV atom)	0.87	0.69	1.41	0.88
ΔH (eV/atom)	−0.257	−0.305	−0.274	−0.327

complete" ω phase (ω''). Finally, the structure parameters were optimized around the minima of the energy (Fig. 2). Calculated atomic parameters for the BOT and ω'' structures are given in Table I.

We use MOPA for studying the bonding between different elements as a function of the atomic displacement z (Fig. 3). The charge and overlap population analyses reveal similar interaction between atoms in both systems. Figure 3 demonstrates several important results. (i) The Ti-Al bond has the highest population overlap with respect to Ti-X and X-Al bonds. (ii) An approaching Ti-Al bond has higher overlap at shorter distances (large z). (iii) Receding Ti-Al bonds show an increase in overlap for the beginning of the collapse and after that a reduction in overlap population. This is evidence of directional bonding between Ti(d) and Al(p) electrons. (iv) The population overlap between receding Ti and X atoms decreases while for approaching X and Al atoms it increases. This confirms the importance of the second nearest neighbor in this type of transformation, which has also been observed

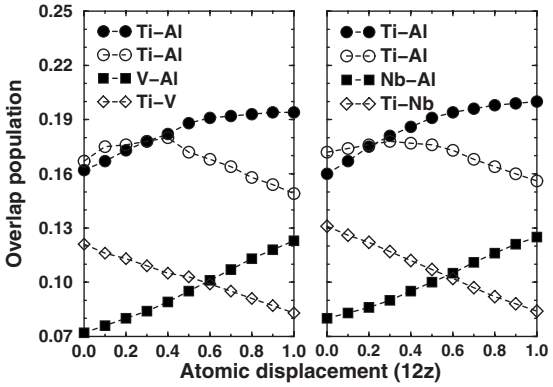

FIG. 3. Population overlap for different bonds as a function of atomic displacement z for Ti_3Al_2V (left) and Ti_3Al_2Nb (right) systems. The approaching (receding) bond is shown with solid (empty) symbols, where approaching (receding) indicates decreasing (increasing) bond length with increasing z.

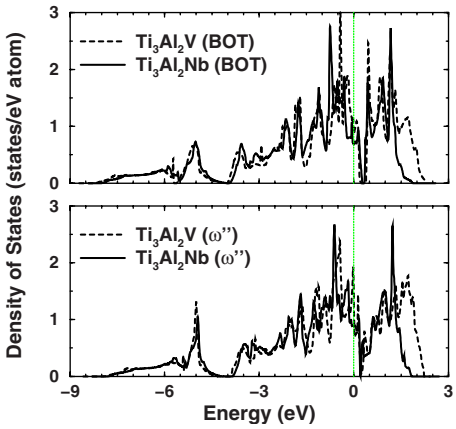

FIG. 4. (Color online) Total DOS of Ti_3Al_2X in BOT and ω'' phases. The Fermi level is shown by the green dotted line.

in the Ni-Al system.[30] The MOPA results are in agreement with x-ray photoelectron spectroscopy[31] studies of Ti-Al and Ti-Al-V alloys that indicate charge transfer from the Al sites toward the transition metal sites.

Figure 4 compares the total density of states (DOS) for $B2$ and ω''-phases of Ti_3Al_2X. For all structures, a low-lying band dominated by s electrons from −8 to −4 eV is separated from other densities by a narrow forbidden gap, which is the result of the hybridization between the s states of the transition metals and Al. It can be seen from the DOS plots that in both the $B2$ and ω'' phases the bonding and antibonding states are separated by a narrow gap and the Fermi level lies in the bonding region. It is also seen that N_{E_f} decreases from V to Nb for both the $B2$ and ω'' phases. This means that the strength of the TM(d)-Al(p) covalent bonding increases. First-principles studies of TM(d)-Al(p) band structures[32,33] confirm that the strength of the TM(d)-Al(p) covalent bonding increases when the TM goes down a column on the periodic table. This is due to the increasing extent of TM(d) orbitals in going from 3d to 5d transition metals. Also it is shown that the bonding strength decreases with increasing numbers of TM(d) electrons.

The heat of formation of alloys is considered useful both for the determination of the existence of compounds and for the insight they give into the strength of the interatomic bonding. To verify the above statements for our systems, we calculate the heat of formation of ternary Ti_3Al_2X structures, besides several binary compounds. In order to determine heats of formation, we first calculated the total energies of elemental Ti, Al, Nb, and V corresponding to their respective equilibrium lattice parameters. At zero temperature, there is no entropy contribution to the free energy and contribution of the zero-point energy is negligible. The heat of formation per atom can be obtained from the following relation:

$$\Delta H = \frac{1}{a+b+c}[E_{\mathrm{Ti}_a\mathrm{Al}_b X_c} - (aE_{\mathrm{Ti}} + bE_{\mathrm{Al}} + cE_X)], \quad (1)$$

where $E_{\mathrm{Ti}_a\mathrm{Al}_b X_c}$ refers to the total energy of the BOT or ω'' phase at equilibrium volume. The heats of formation are given in Table I.

Since in ω-type atomic displacements the number of nearest and second nearest neighbors is changing, we choose a structure in which TM-Al bonds can exist as the first and second nearest neighbors. By replacing Al atoms in the fourth plane of Fig. 1(d) with Ti atoms, such a configuration can be created. The calculated values for an underlying bcc structure confirm that Ti_2Al (−0.244 eV/atom) has lower heat of formation with respect to Nb_2Al (−0.125 eV/atom) and V_2Al (−0.084 eV/atom). That is, the TM-Al bond strength increases from V to Nb to Ti, in agreement with band structure results. The underlying bcc structures are unstable with respect to the ω-type displacements. Indeed, the lowest-energy configuration corresponds to complete collapse of the planes [Fig. 1(c)] and has 0.071, 0.070, and 0.018 eV/atom less energy for Ti_2Al, Nb_2Al, and V_2Al, respectively. Calculated heats of formation not only show a similar pattern of the strength among TM-Al bonds for this new structure, but also confirm that the TM-Al bond is more stable at shorter distances with respect to the original BOT structure. Similar calculations for Ti_2Nb (0.050 eV/atom) and Ti_2V (0.122 eV/atom) confirm that these structures are unstable. The above findings are in agreement with near neighbor Lennard-Jones potentials for Ti-Al and Nb-Al pairs,[34] and with the bcc Ti-Nb interaction parameters derived by Moffat and Kattner.[35] These parameters indicate that the most stable bond is Ti-Al, the Nb-Al is slightly less stable, and the Ti-Nb bond is weakly unstable; with the Ti-Al bond being more stable than Nb-Al at shorter distances.

Note that in the Ti_3Al_2Nb alloy the energy difference between the BOT and ω'' phases is bigger than in the Ti_3Al_2V case. This can be explained based on the strength of the different TM-Al bonds. In the BOT structure, the X and Al atoms are second nearest neighbors. In the ω'' phase the X-Al bond length is approximately equal to the average of the first and second nearest neighbor distances. From Fig. 3, it is easy to see that in ω-type atomic displacements the overlap population between approaching X and Al atoms is significantly increased, while it is decreased for Ti and X atoms. Since the Nb-Al bond is stronger than V-Al (especially at shorter distances), the reduction in energy from the BOT to the ω'' phase in Ti_3Al_2Nb is much bigger than in the Ti_3Al_2V system. Similar arguments can be used to explain why Ti_3Al_2Nb has the lowest heat of formation (Table I).

IV. STABILITY OF BOT AND ω'' STRUCTURES

In the BOT structure, the Ti atom in the third plane has X (fourth plane) and Al (second plane) atoms as first nearest neighbors. According to the results of the previous section the Ti-Al bond is stronger than the Ti-X bond. Consequently, the BOT structure cannot be stable with respect to ω-type atomic displacements. We demonstrate this statement with another approach. Ti-X bonds are the weakest bonds in our system; therefore, if the number of Ti-X bonds is reduced then the underlying bcc structure should be stabilized. We replaced the X atoms in the fourth plane with Al atoms [Fig. 1(d)] and calculated the energy of the system as a function of the atomic displacements. The total energy vs atomic displacements for the TiAl structure showed that the $B2$ structure and ω phase are separated by an energy barrier (Fig. 5). It is important to mention that the $B2$ phase of TiAl has not yet been observed.

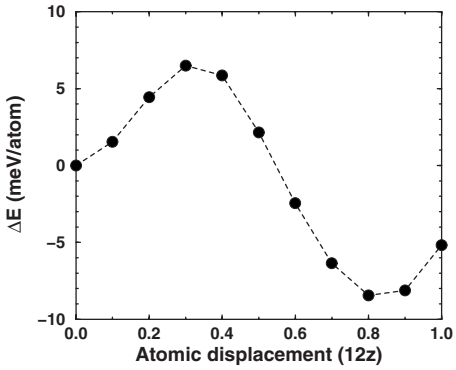

FIG. 5. Total energy vs ω-type atomic displacement for the $B2$ TiAl system. The $B2$ and ω phases are separated by a barrier which is absent in the Ti_3Al_2X system.

Within the $B2$ structure, each Ti atom has eight Al atoms as a first nearest neighbor. By displacing the atoms toward an ω-type structure, the number of first nearest neighbors is changing. For example, for Ti atoms in the first plane [Fig. 1(d)], six of the nearest neighbor Al atoms increase their distance while the two other Al atoms, located in the fourth plane, remain the same. On the other hand, the distance between the Ti and Al atoms in the collapsing planes (second and third) decreases. Consequently, in the ω-phase transformation, some of the atoms remain stationary while the distances between the rest of the atoms are changed (increased or decreased). The Ti-Al is the most stable bond and the Ti-X bond is the unstable one, with the Ti-Al bond being more stable at shorter distances (with respect to their distance in the $B2$ structure). Thus, when the distance between the Ti atoms in the first plane and Al atoms in the second and sixth planes, and Al atoms in the fourth plane and Ti atoms in the third and fifth planes increases, the energy of the system also increases. It is this interaction which leads to the barrier separating the $B2$ structure from the ω phase (Fig. 5). By replacing the Al atoms in the fourth plane [Fig. 1(d)] with Nb or V atoms [Fig. 1(a)] the number of receding Ti-Al bonds are reduced, replaced by unstable Ti-X bond. Now, focus on Ti atom at the third plane (or fifth plane) in Fig. 1(a). Ti atoms are now interacting with Al and X atoms, which are located at two different sides (second and fourth planes) of the Ti atoms. Movement of the atoms in ω-type displacements reduces the Ti-Al distance and at the same time increases the Ti-X distance, which favors strong bonding and therefore reduces the energy of the system.

Summarizing the results, according to the above discussion, one can say the following. The presence of the energy barrier in $B2$ TiAl is due to receding nearest neighbor Ti-Al bonds, which are more stable at shorter distances. By substituting the Al atoms in the middle (fourth) plane by Nb or V

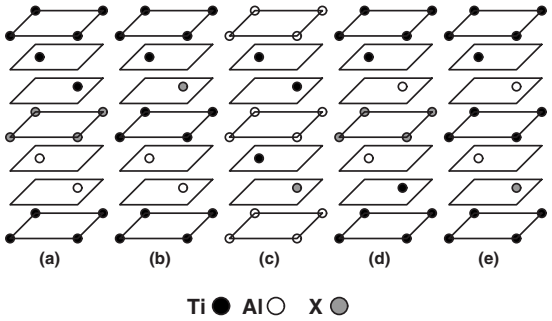

FIG. 6. Different rearrangements of the atoms for Ti_3Al_2X alloy with an underlying bcc structure.

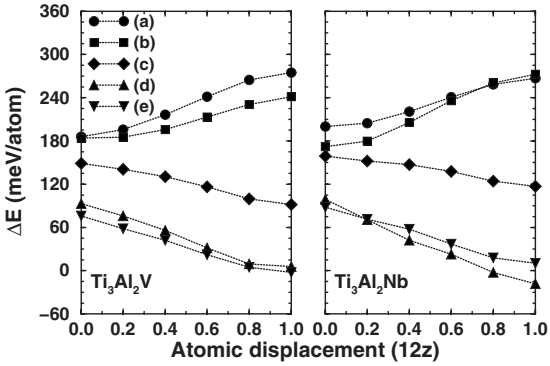

FIG. 7. Total energy vs ω-type atomic displacement for different arrangements of the atoms (Fig. 6). Value of E_0 is equal to the BOT structure of each system.

atoms, the number of the receding Ti-Al bonds is reduced to half of the original value, which makes the energy barrier disappear. However, the new Ti-X bonds are unstable and, in contrast to the Ti-Al bonds, prefer that the bond expands. Therefore these new bonds destabilize the BOT structure completely (absence of the energy barrier for the BOT structure). The ω'' phase is a structure created from the competition between these bonds.

V. CHEMICAL ORDERING PROCESS

To understand the effect of the chemical ordering on the stability of the BOT structure with respect to the ω-type atomic displacement, several different structures have been investigated (Fig. 6). The lattice parameters for each rearranged structure are optimized. If the calculated energy for the BOT Ti_3Al_2X (X=Nb, V) structure is shown as E_0, the following sequence of energy holds for the structures shown in Fig. 6: $E_0 < E_e < E_d < E_c < E_b < E_a$. In Table II, the energy and numbers of Ti-Al and Ti-X bonds as the first nearest neighbors for different atomic arrangements are shown. We found that there is a direct relation between the number of Ti-Al bonds and the energy of the underlying bcc phases. Structures with a higher number of Ti-Al bonds have a lower energy. Using the results of the previous section we can explain the energy sequence for the different structures. Recall that the Ti-Al bond is stronger than the Ti-X and Ti-Al bonds are stronger at shorter distances, relative to their positions in rearranged structures. Therefore, one expects to see instability of the structures with more Ti-Al bonds toward the ω phase. In this way, the Ti-Al bond is reducing its energy. This statement is again in agreement with the results of our calculations (Fig. 7). According to our results, the structures in Figs. 6(c)–6(e), and the BOT structure are showing instability toward an ω-type structure (Figs. 6 and 7).

TABLE II. Difference between energy of rearranged and BOT structures and number of first nearest neighbor Ti-Al and Ti-X (X =Nb, V) bonds.

Structure	ΔE (meV/atom) Ti_3Al_2V	ΔE (meV/atom) Ti_3Al_2Nb	Ti-Al	Ti-X
(a)	186	200	7	5
(b)	184	172	8	6
(c)	149	159	9	5
(d)	93	99	10	2
(e)	76	88	11	3
(BOT)	0	0	16	8

Based on the first principles results (Fig. 7), the only possible way that structures (a) and (b) can reduce their energies are for the atoms to rearrange (diffuse) to another low-energy configuration. On the other hand, for structures (c), (d), and (e), the energy of these systems could be reduced by undergoing a (nondiffusive) structural transformation to a complete ω structure (Fig. 7). However, the total energies of these complete ω structures are different. These energies are higher than the energy of the ω'' Ti_3Al_2X structure. Thus, after ω-type transformations, the energy of these system can be further reduced by diffusion and displacement of the atoms (e.g., to the ω'' Ti_3Al_2X structure). That is, the calculations shown in Fig. 7 reveal the possible paths (diffusive and nondiffusive) for the Ti_3Al_2X system which have been observed in different experiments.[2,12,13] Therefore, chemical orderings of the atoms play a crucial rule in the stability of the BOT structure with respect to the ω-phase transformation.

VI. SUMMARY

We have performed first-principles calculations to study the formation of the ω phase in ordered $B2$ Ti_3Al_2Nb and Ti_3Al_2V alloys. We used the total density of states and employed Mulliken overlap population analysis to study the interaction and hybridization between different types of atoms and their effects on formation of the ω phase. Calculation of the heats of formation for several different compounds gave us an estimate for the strength of existing bonds. We find that Ti-Al is the strongest bond and that the Ti-X bond is unstable. It was shown that the barrier in the TiAl transformation which separates the $B2$ and ω phases is due to receding Ti-Al bonds. When some Al atoms are replaced by Nb or V atoms, the number of receding Ti-Al bonds is reduced, and they are replaced by Ti-X bonds, which are weaker than

Ti-Al bonds, this causes the instability in the BOT structure against the ω'' phase.

In addition, the importance of chemical ordering in the stability of the underlying bcc structure of Ti_3Al_2X was discussed. We showed that, with a simple argument based on the number of Ti-Al and Ti-X bonds in each system, one can predict the stability of each rearranged structure. The results of the first-principles calculations for the lattice parameters of Ti_3Al_2X are in agreement with experiment.

ACKNOWLEDGMENTS

This work was carried out under the auspices of the Advanced Research Program of the State of Texas and the National Nuclear Security Administration of the U.S. Department of Energy at Los Alamos National Laboratory under Contract No. DE-AC52-06NA25396. The generous amounts of computer time provided by Texas Tech's High Performance Computer Center were much appreciated.

*m.sanati@ttu.edu

[1] *Proceedings of the International Symposium on Intermetallic Compounds*, edited by O. Izumi (JIM Publications, Sendai, Japan, 1991).
[2] L. A. Bendersky, W. J. Boettinger, B. P. Burton, and F. S. Biancaniello, Acta Metall. Mater. **38**, 931 (1990).
[3] F. A. Sadi and C. Servant, Philos. Mag. A **80**, 639 (2000).
[4] F. A. Sadi and C. Servant, Z. Metallkd. **91**, 504 (2000).
[5] C. B. Shoemaker, D. P. Shoemaker, and L. A. Bendersky, Acta Crystallogr., Sect. C: Cryst. Struct. Commun. **46**, 374 (1990).
[6] T. H. Yu and C. H. Koo, Mater. Sci. Eng., A **239-240**, 694 (1997).
[7] R. Strychor, J. C. Williams, and W. A. Soffa, Metall. Trans. A **19**, 225 (1988).
[8] C. P. Chang and M. H. Loretto, Philos. Mag. A **63**, 389 (1991).
[9] T. Ahmed and H. M. Flower, Mater. Sci. Eng., A **152**, 31 (1992).
[10] P. Tsakiropoulos and G. Shao, Mater. Sci. Eng., A **375-377**, 201 (2004).
[11] G. Shao and P. Tsakiropoulos, Mater. Sci. Eng., A **329-331**, 914 (2002).
[12] G. Shao, P. Tsakiropoulos, and A. P. Miodownik, Mater. Sci. Eng., A **216**, 1 (1996).
[13] G. Shao, A. P. Miodownik, and P. Tsakiropoulos, Philos. Mag. A **71**, 1389 (1995).
[14] S. K. Sikka, Y. K. Vohra, and R. Chidambaran, Prog. Mater. Sci. **27**, 245 (1982).
[15] D. Banerjee, T. K. Nandy, and A. K. Gogia, Scr. Metall. **21**, 597 (1987).
[16] Computer code VASP, at http://cms.mpi.univie.ac.at/vasp
[17] G. Kresse and J. Hafner, Phys. Rev. B **47**, 558 (1993).
[18] G. Kresse and J. Furthmüller, Phys. Rev. B **54**, 11169 (1996).
[19] G. Kresse and D. Joubert, Phys. Rev. B **59**, 1758 (1999).
[20] D. P. Ordejón, E. Artacho, and J. M. Soler, Int. J. Quantum Chem. **65**, 453 (1997).
[21] E. Artacho, D. Sánchez-Portal, P. Ordejón, A. García, and J. M. Soler, Phys. Status Solidi B **215**, 809 (1999).
[22] J. P. Perdew, in *Electronic Structure of Solids'91*, edited by P. Ziesche and H. Eschring (Akademie-Verlag, Berlin, 1991), p. 11.
[23] J. P. Perdew, K. Burke, and M. Ernzerhof, Phys. Rev. Lett. **77**, 3865 (1996).
[24] D. Vanderbilt, Phys. Rev. B **41**, 7892 (1990).
[25] G. Kresse and J. Furthmüller, Comput. Mater. Sci. **6**, 15 (1996).
[26] H. J. Monkhorst and J. D. Pack, Phys. Rev. B **13**, 5188 (1976).
[27] N. Troullier and J. L. Martins, Phys. Rev. B **43**, 1993 (1991).
[28] O. F. Sankey and D. J. Niklewski, Phys. Rev. B **40**, 3979 (1989); O. F. Sankey, D. J. Niklewski, D. A. Drabold, and J. D. Dow, *ibid.* **41**, 12750 (1990).
[29] A. A. Demkov, J. Ortega, O. F. Sankey, and M. P. Grumbach, Phys. Rev. B **52**, 1618 (1995).
[30] M. Sanati, R. C. Albers, and F. J. Pinski, J. Phys. C **13**, 5387 (2001).
[31] S. Diplas, J. F. Watts, P. Tsakiropoulos, G. Shao, G. Beamson, and J. A. D. Matthew, Surf. Interface Anal. **31**, 734 (2001).
[32] D. J. Singh, in *Intermetallic Compounds: Principles and Practice*, edited by J. H. Westbrook and R. L. Fleischer (Wiley, New York, 1995), Vol. 1, p. 127.
[33] Q. M. Hu, R. Yang, D. S. Xu, Y. L. Hao, D. Li, and W. T. Wu, Phys. Rev. B **68**, 054102 (2003).
[34] M. Enomoto and H. Harada, Metall. Trans. A **20**, 649 (1989).
[35] D. L. Moffat and U. R. Kattner, Metall. Trans. A **19**, 2389 (1988).